Hydrol. Earth Syst. Sci. Discuss., 8, 5559–5604, 2011
www.hydrol-earth-syst-sci-discuss.net/8/5559/2011/
doi:10.5194/hessd-8-5559-2011

Hydrology and Earth System Sciences Discussions

Influence of soil parameters on the skewness coefficient of the annual maximum flood peaks

A. Gioia[1], V. Iacobellis[1], S. Manfreda[2], and M. Fiorentino[2]

[1]Dipartimento di Ingegneria delle Acque e di Chimica, Politecnico di Bari, Italia
[2]Dipartimento di Ingegneria e Fisica dell'Ambiente, Università degli Studi della Basilicata, Italia

Received: 10 April 2011 – Accepted: 21 April 2011 – Published: 14 June 2011

Correspondence to: A. Gioia (a.gioia@poliba.it)

Published by Copernicus Publications on behalf of the European Geosciences Union.

Abstract

Understanding the spatial variability of key parameters of flood probability distributions represents a strategy to provide insights on hydrologic similarity and building probabilistic models able to reduce the uncertainty in flood prediction in ungauged basins. In this work, we exploited the theoretically derived distribution of floods TCIF (Gioia et al., 2008), based on two different threshold mechanisms associated respectively to ordinary and extraordinary events. The model is based on the hypotheses that ordinary floods are generally due to rainfall events exceeding a threshold infiltration rate in a small source area, while the so-called outlier events, responsible of the high skewness of flood distributions, are triggered when severe rainfalls exceed a storage threshold over a large portion of the basin. Within this scheme, a sensitivity analysis was performed in order to analyze the effects of climatic and geomorphologic parameters on the skewness coefficient. In particular, the analysis was conducted investigating the influence on flood distribution of physical factors such as rainfall intensity, soil infiltration capacity, and basin area, in order to provide insights in catchment classification and process conceptualization.

1 Introduction

The understanding of processes control on the shape of the flood frequency distribution is essential to extrapolate reliable at-site predictions to large return periods and to define meaningful similarity indicators between catchments for flood frequency estimation in ungauged catchments (Merz and Bloschl, 2009). These physical interconnections may be explored using an upward approach (or model based), where a stochastic rainfall model is coupled with a runoff model based on derived distribution approach (Eagelson, 1972; Raines and Valdes, 1993; Gottschalk and Weingartner, 1998; Fiorentino and Iacobellis, 2001; De Michele and Salvadori, 2002; Franchini et al., 2005; Bocchiola and Rosso., 2009) or Monte Carlo simulations (e.g., Beven, 1987; Loukas, 2002; Blazkova and Beven, 2002; Fiorentino et al., 2007).

HESSD
8, 5559–5604, 2011

The literature proposes a number of schemes and procedures for the theoretical derivation of flood probability distributions. Models differ in the basic assumptions on the rainfall probability distributions as well as the scheme of the runoff model which is either deterministic or random, according to different authors. Among others, Sivapalan et al. (1990) accounted for the effect of different mechanisms of runoff generation (infiltration excess and saturation excess). Iacobellis and Fiorentino (2000) introduced the partial contributing area as a random variable and considered only one runoff threshold mainly associated either to infiltration excess in arid basins or to saturation excess in humid basins.

Most of the derived distributions developed so far are based on a single runoff generation scheme, but this may represent a limitation in the description of runoff production. Moreover, it is not always clear how well the single component describe the complex dynamics of flood formation occurring within the river basin. In fact, the runoff processes are felt to be a relevant component in the description of flood generation processes along with the rainfall forcing that generally can be easily measured and described by a given probability distribution.

The effects of runoff thresholds have received particular attention in flood frequency analysis in last few years (e.g., McGrath et al., 2007). Kusumastuti et al. (2007) focused on catchment storage and derived the flood frequency distributions by Monte Carlo simulations, using a non-linear conceptual rainfall-runoff model. Struthers and Sivapalan (2007) illustrate the impact of heterogeneity associated with threshold non-linearities in the storage-discharge relationship associated with the rainfall-runoff process upon flood frequency behaviour. They introduced two storage thresholds, namely a field capacity storage and a catchment storage capacity, that identify two different flood frequency “regions”. The return period associated with the transition between these regions is directly related to the frequency of threshold exceedence.

The detection of the dominant processes in the flood formation represents the main way for building models capable to reproduce real processes and reduce the uncertainty on flood prediction with particular attention to ungauged basins. In this context, the presence of different runoff generation processes, such as the saturation excess and the infiltration excess mechanisms, under different climatic conditions and the dynamics which control the transition between the two schemes, provides interesting insights, useful to find similarities and differences among river basins and among their processes for classification and regionalization. With this aim, this paper describes the effect of different runoff production mechanisms on the generation of ordinary and extraordinary flood events exploiting the theory on derived flood probability distribution. In this paper, the TCIF flood frequency distribution (Gioia et al., 2008) is exploited to analyse the effects of climatic and geomorphologic parameters on statistical flood moments and in particular on the skewness coefficient.

Some interesting results in this direction were already obtained by Iacobellis et al. (2002) exploiting the theoretical model proposed by Iacobellis and Fiorentino (2000). In particular, they explored the spatial variability of the coefficient of variation of annual maximum floods. They derived a theoretical dependence between the coefficient of variation (C_v) and the abstraction characteristics at the basin scale, the basin area and rainfall parameters. Their findings highlighted that C_v scales with the basin area following distinct behaviour that is influenced by the dominant runoff mechanisms. In particular, C_v decreases with area when the infiltration excess mechanism dominates, while C_v increases with area in humid and vegetated basins where saturation excess runoff take place.

The focus here is on the definition of a relationship between physical basin characteristics and the skewness coefficient (C_s). C_s can vary vastly in catchments, which apparently exhibit similar flood behaviour. This may be due to the interaction of temporal varying observation periods and climate fluctuations, single extreme events and observation errors (Merz and Bloschl, 2009). Following the conceptual method proposed by McCuen and Smith (2008), the flood skew estimation involves rainfall skew

HESSD
8, 5559–5604, 2011

and watershed and channel storage. In their scheme, rainfall skew represents an upper bound on the population of runoff skew and flood skew decreases from the rainfall skew for the same location as storage increases. We demonstrate that, introducing two different runoff thresholds, based on permeability and soil storage capacity, flood skew can be much larger than rainfall skew. Indication on the physical controls on this specific parameter is essential for reliably extrapolating at-site statistics to large return periods.

2 Theoretically derived flood frequency distribution (TCIF model)

The TCIF distribution was derived by Gioia et al. (2008) under the hypothesis that in natural basins different mechanisms of runoff generation may coexist, being in turn responsible of the peak flow, depending on the characteristics of the rainfall event and on the antecedent moisture conditions. The two mentioned mechanisms were defined as:

- L-type (frequent) response, occurring when rainfall intensity ($i_{a,\tau}$) exceeds a lower threshold $f_{a,L}$, and responsible of ordinary floods likely produced by a relatively small portion of the basin a_L; the L-type (frequent) peak unit runoff is: $u_{a,L} = \xi\,(i_{a,\tau} - f_{a,L})$.
- H-type (rare) response, occurring when rainfall intensity exceeds a higher threshold $f_{a,H}$, and providing extraordinary floods mostly characterized by larger contributing areas a_H; the H-type (rare) peak unit runoff is: $u_{a,H} = \xi\,(i_{a,\tau} - f_{a,H})$.

Other assumptions of the TCIF distribution model are that rainfall and infiltration, averaged in space and time, scale with the contributing area with the following relationships:

$$E\left[i_{a,\tau}\right] = i_1\, a^{-\varepsilon} = E\left[i_{A,\tau}\right] (a/A)^{-\varepsilon} \tag{1}$$

$$f_{a,L} = f_{A,L}\left(a_L/A\right)^{-\varepsilon_L} \tag{2}$$

HESSD

8, 5559–5604, 2011

Influence of soil parameters on the skewness coefficient

A. Gioia et al.

$$f_{a,H} = f_{A,H}\left(a_H/A\right)^{-\varepsilon_H} \tag{3}$$

The rainfall intensity is considered Weibull distributed (with shape parameter k) and the contributing areas a_L and a_H have a continuous part, Gamma distributed, and a spike of discrete probability for $a = A$ total basin area. The scale parameter is β and position parameters are $\alpha_L = r_L A/\beta$ and $\alpha_H = r_H A/\beta$ dependent by the two dimensionless parameters $r_L = E[a_L]/A$ and $r_H = E[a_H]/A$ with $r_H \geq r_L$.

Assuming that L-type and H-type events are independent and that both rates of occurrence are Poisson distributed, the overall process of exceedances is also a Poisson process; the cumulative probability distribution, $\mathrm{CDF}_{Q\mathrm{p}}(q_\mathrm{p})$, of the annual maximum flood peak $q_\mathrm{p} = Q + q_\mathrm{o}$, with q_o the base flow, and its probability density function (e.g. Iacobellis et al., 2011) are:

$$\mathrm{CDF}_{Q_\mathrm{p}}(q_\mathrm{p}) = \exp\left\{-\Lambda_L\left[\int_0^A g(a_L)\exp\left(-\frac{\left((q_\mathrm{p}-q_\mathrm{o})/(\xi a_L)+f_{a,L}\right)^k-\left(f_{a,L}\right)^k}{\left(E[i_{a_L,\tau}]/\Gamma(1+1/k)\right)^k}\right)da_L\right]\right\}+ \tag{4}$$

$$+\exp\left\{-\Lambda_H\left[\int_0^A g(a_H)\exp\left(-\frac{\left((q_\mathrm{p}-q_\mathrm{o})/(\xi a_H)+f_{a,H}\right)^k-\left(f_{a,H}\right)^k}{\left(E[i_{a_H,\tau}]/\Gamma(1+1/k)\right)^k}\right)da_H\right]\right\}$$

$$\mathrm{PDF}_{Q_\mathrm{p}}(q_\mathrm{p}) = \mathrm{CDF}_{Q_\mathrm{p}}(q_\mathrm{p})\left[\Lambda_L\left\{\int_0^A g(a_L)\frac{k}{(\xi a_L)\left(E[i_{a_L,\tau}]/\Gamma(1+1/k)\right)^k}\left(\frac{(q_\mathrm{p}-q_\mathrm{o})}{(\xi a_L)}+f_{a,L}\right)^{k-1}\right.\right. \tag{5}$$

$$\exp\left(-\frac{\left((q_\mathrm{p}-q_\mathrm{o})/(\xi a_L)+f_{a,L}\right)^k-\left(f_{a,L}\right)^k}{\left(E[i_{a_L,\tau}]/\Gamma(1+1/k)\right)^k}\right)da_L$$

HESSD
8, 5559–5604, 2011
Influence of soil parameters on the skewness coefficient
A. Gioia et al.

$$+\Lambda_H \left\{ \int_0^A g(a_H) \frac{k}{(\xi a_H)\left(E[i_{a_H,\tau}]/\Gamma(1+1/k)\right)^k} \left(\frac{(q_p - q_o)}{(\xi a_H)} + f_{a,H} \right)^{k-1} \right.$$

$$\left. \exp\left(- \frac{\left((q_p - q_o)/(\xi a_H) + f_{a,H} \right)^k - (f_{a,H})^k}{\left(E[i_{a_H,\tau}]/\Gamma(1+1/k)\right)^k} \right) da_H \right\} \Bigg]$$

ξ is a constant routing factor, Λ_L and Λ_H are the mean annual number of independent flood events for the L-type and the H-type events; $E[i_{a_L,\tau}]$ and $E[i_{a_H,\tau}]$ are respectively the average rainfall intensity with respect to contributing areas a_L and a_H; $g(a_L)$ and $g(a_H)$ are respectively the probability density functions of the L-type and H-type contributing areas.

Furthermore, the following relationships hold:

$$\Lambda_H = \Lambda_p \exp\left(- \frac{f_{A,H}^k}{E[i_{A,\tau}^k]} \right) \tag{6}$$

and

$$\Lambda_q = \Lambda_L + \Lambda_H = \Lambda_p \exp\left(- \frac{f_{A,L}^k}{E[i_{A,\tau}^k]} \right) \tag{7}$$

Assuming the rainfall intensity Gumbel distributed, $k=1$ and:

$$E\left[i_{A,\tau}^k\right] = E\left[i_{A,\tau}\right] = I_A = I_1 A^{-\varepsilon} \tag{8}$$

with I_1 the rainfall intensity per unit contributing area.

In Gioia et al. (2008) and Iacobellis et al. (2011) particular attention was paid to the dynamics of runoff source areas by revealing the scaling behaviour of the runoff

HESSD
8, 5559–5604, 2011

thresholds ($f_{A,L}$ and $f_{A,H}$). In particular investigating the different mechanisms of runoff production that coexist in humid climates, they found that the scaling behaviour of the H-type (rare events) runoff threshold corresponds to a storage threshold, while the L-type (frequent events) runoff threshold corresponds to a constant infiltration rate. The H-type (rare events) response arises only when an intense and persistent rainfall of significant areal extension exceeds a water storage capacity over large and more or less vegetated hillslopes; on the other hand the L-Type response could be associated to a saturation excess mechanism in humid climates.

In order to keep trace of the different role of permeability and soil storage capacity in the proposed sensitivity analysis, we characterized the two runoff thresholds considering the lower threshold $f_{A,L}$ as associated to the spatial average of soil permeability in saturated conditions, ϕ,

$$f_{A,L} \cong \phi. \tag{9}$$

Then, we consider the soil water storage capacity averaged in space and over the basin lag-time, which scales with basin area as

$$W_A = W_1 A^{-0.5}, \tag{10}$$

the higher runoff threshold can be evaluated as:

$$f_{A,H} \cong \phi + W_A. \tag{11}$$

When rainfall exceeds the lower permeability threshold, a small source area a_L corresponding to the first (L-type) component is activated with mean annual number of exceedances equal to $\Lambda_q = \Lambda_H + \Lambda_L$ (see Eq. 7). Instead the exceedances of the second runoff threshold (equal to the permeability plus soil storage capacity) characterizes the activation of a larger source area a_H corresponding to the second (H-type) component with mean annual number of exceedance equal to Λ_H (see Eq. 6).

In order to provide a general framework for the physical interpretation of results of the sensitivity analysis, in Table 1 we consider the range of variability of each threshold

HESSD
8, 5559–5604, 2011

Influence of soil parameters on the skewness coefficient

A. Gioia et al.

parameter (ϕ and W_A) divided in three classes: low, medium and high. Then, a qualitative evaluation of the occurrences of the two different components is derived from Eqs. (6) and (7). In fact, the occurrence of events of the 1st and 2nd components is related to the probability of rainfall to exceed the corresponding thresholds. For each cell of Table 1, we indicate in the upper left corner the frequency of the L-type component, corresponding to the probability $P(i > \phi)$, and in the bottom right corner the frequency of the H-type component, corresponding to the probability $P(i > \phi + W_A)$. Thus, for low values of permeability, the probability of rainfall to exceed the first runoff threshold is high; increasing permeability, the number of rainfall events that exceeds the first runoff threshold becomes occasional for medium ϕ and rare for high ϕ. Then, if the soil storage assumes values belonging to the lower class, the number of the exceedances of the second runoff threshold is frequent, occasional and rare as it is in the range of variation of permeability; increasing the value of the soil storage, the number of the exceedances becomes occasional, rare, very rare and extremely rare.

Following the above arguments, we report in Table 2 the expected behaviour of a basin in terms of presence and relevance of the two runoff components. For low values of the soil storage (W_A), the two runoff thresholds are close (see Eqs. 9 and 11), then, it is possible to recognize only one component (L-type) of the theoretical model; when the soil storage increases the second component may become distinguishable; in particular for medium values of the soil storage, the first component may be not relevant if the permeability is low (only the H-type component is present); on the other hand, if the permeability is high the second runoff threshold assumes very high values then the second component may become not observable. Even for high values of soil storage, increasing the values of permeability the frequency of exceedances of the second runoff threshold will be so low that the second component may be not observable and not significant for return periods of technical interest.

In order to investigate on the role that the combination of the two processes may have on the shape of the flood frequency curve, the sensitivity analysis was carried out changing the rate of L-type and H-type events over a broad range that embraces all

HESSD
8, 5559–5604, 2011

possible cases identified above. Those values, given only qualitatively in Tables 1 and 2, are described in Table 3 in terms of mean annual number of flood events Λ_q, equal to the number of rainfall events that exceed the first threshold ϕ, and the average annual number of flood events Λ_H exceeding also the second threshold $W_A+\phi$. According to the variability of Λ_q observed in Southern Italy (see Iacobellis et al., 2011), we considered values of 5, 10 and 20 flood events per year as representative of, respectively, low, medium and high frequency. For the occurrence of the second runoff threshold we considered six values obtained adopting a fixed ratio between Λ_H and Λ_q (1/3, 1/10, 1/20, 1/50, 1/200 and 1/1000).

In the hypothesis of rainfall intensity Gumbel distributed, with $k=1$, and replacing Eqs. (8) and (11) in Eq. (6) we obtain:

$$\frac{\phi+W_A}{I_A} = -\ln\left(\frac{\Lambda_H}{\Lambda_p}\right) \tag{12}$$

Replacing Eqs. (8) and (9) in Eq. (7):

$$\frac{\phi}{I_A} = -\ln\left(\frac{\Lambda_q}{\Lambda_p}\right); \tag{13}$$

and combining Eqs. (12) and (13):

$$\frac{W_A}{I_A} = -\ln\left(\frac{\Lambda_H}{\Lambda_q}\right). \tag{14}$$

Following Eq. (14), the ratio Λ_H/Λ_q depends only on W_A/I_A. Moreover, following Eqs. (13) and (12), for a fixed value of Λ_p, Λ_q depends only on the ratio ϕ/I_A and Λ_H depends only on the ratio $(\phi+W_A)/I_A$. Therefore for a fixed value of Λ_p, of the ratio Λ_H/Λ_q and of Λ_q it is possible to calculate the corresponding values of ϕ/I_A and W_A/I_A. In Table 4 we report the values of the dimensionless ratios ϕ/I_A obtained by means of Eq. (13), for $\Lambda_p=21$ and different values of Λ_q and Λ_H. Table 4 reports also

HESSD
8, 5559–5604, 2011

Influence of soil parameters on the skewness coefficient

A. Gioia et al.

the values of the dimensionless ratio W_A/I_A obtained by means of Eq. (14) for different values of Λ_q and Λ_H. In both cases the corresponding values of Λ_H are those reported in Table 3 for the same Λ_q-row and Λ_H/Λ_q-column. For known values of ϕ/I_A and W_A/I_A, ϕ and W_A can be obtained according to values of I_1, A, and ε, which, following Eq. (8), provide I_A. Other parameters affecting the TCIF cumulative distribution function in Eq. (4) are the ratios of the average contributing areas r_L and r_H during a L-type and H-type event, respectively.

The sensitivity analysis was performed by numerically evaluating the TCIF cumulative distribution function and its probability density function, $\mathrm{PDF}_{\mathrm{Qp}}$ (q_p), for different sets of parameters $\Lambda_p, I_1, A, \varepsilon, r_L, r_H, \Lambda_H/\Lambda_q$ and Λ_q and keeping constant the values of the following other parameters:

- the routing factor ξ, assumed equal to 0.7, as in Iacobellis and Fiorentino (2000);
- the shape parameter β of the gamma distribution of the contributing areas assumed equal to 4 as in Iacobellis and Fiorentino (2000);
- the exponents ε_L and ε_H of the power low relationship between infiltration losses and contributing area assumed respectively equal to 0 and 0.5 as reported in Gioia et al. (2008).

The skewness coefficient of the distribution was evaluated, by solving numerically the equation:

$$C_\mathrm{s} = \frac{\int_{-\infty}^{+\infty} (q_\mathrm{p} - \mu(q_\mathrm{p}))^3 \mathrm{PDF}_{Q_\mathrm{p}}(q_\mathrm{p})\, d q_\mathrm{p}}{\left[\int_{-\infty}^{+\infty} (q_\mathrm{p} - \mu(q_\mathrm{p}))^2 \mathrm{PDF}_{Q_\mathrm{p}}(q_\mathrm{p})\, d q_\mathrm{p}\right]^{3/2}}; \quad \text{with } \mu(q_\mathrm{p}) = \int_{-\infty}^{+\infty} q_\mathrm{p}\, \mathrm{PDF}_{Q_\mathrm{p}}(q_\mathrm{p})\, d q_\mathrm{p} \tag{15}$$

In order to provide a structured analysis of the influence of physical factors such as permeability and soil storage on the TCIF distribution, and its skewness, the values of Λ_H and Λ_q were selected on the basis of Table 3, hence, for fixed values of the ratio

Λ_H/Λ_q. Then, in order to analyze the role of permeability and soil storage we used the ratios ϕ/I_A and W_A/I_A shown in Table 4.

For the other parameters of the TCIF distribution, we assigned a range of variability coherent with observed values on a set of river basins in Southern Italy investigated in previous studies (Gioia et al., 2008; Fiorentino et al., 2011; Iacobellis et al., 2011). In particular, Λ_p ranges from 21 to 75 (event/yr); I_1 aries from 10 to 50 mm h^{-1}; A ranges from 10 to 500 km^2; ε varies from 0.3 to 0.4; r_L and r_H range from 0 to 1 with $r_H >= r_L$. We first report results for the entire observed variability of r_L, r_H, basin area A and rainfall intensity I_1 and for the fixed values $\Lambda_p = 21$ and $\varepsilon = 0.3$. Significant results obtained for different values of Λ_p and ε are also discussed, provided that changing these last two parameters do not affect qualitatively the results and their implications on the paper focus which is the understanding of the role of permeability and soil storage on the presence of two runoff components and on the flood distribution skewness. We did not introduce any change of parameters ξ and β because in all the application performed on real cases in previous studies they did not show any variability. In the present application, the base flow q_o is set to zero, because in the TCIF model q_o is added as a constant factor to the peak flow and hence does not affect the peak flow distribution. Finally, the analysis does not account for changes in the shape parameter, k, of the rainfall pdf (i.e. of rainfall skewness) which is left to further research.

3 Results and discussion

Results of the sensitivity analysis are described in the present section with particular emphasis on the skewness coefficient of the theoretical distributions. Results are reported in the form of growth curve probability plots. Moreover, the skewness coefficients obtained with different parameter combinations are summarized in tabular form (see Tables 5–9). According to the index flood method (NERC, 1975), the growth curve represents by definition the cdf of the growth factor

$$K_x = x/E[x] \quad (16)$$

whose distribution is independent from the expected value. The growth curve depends on scale factor and shape factor of the distribution. The TCIF arises as a distribution of annual maximum of a Poisson compound process just as many other distributions of extreme values (e.g. GEV, TCEV). The coefficient of variation of such distributions, controlling the scale factor, mainly depends on Λ_q. Thus, the representation of TCIF growth curves characterized by the same value of Λ_q and different values of the other parameters, allows the identification of shape changes on the growth curve, with direct reference to the return period of the growth factor. The return period (defined as the inverse of the probability that a given event will be exceeded) is reported on the y-axis in a log scale limiting the range of values to those of technical interest (1–1000 yr).

Figures 1–13 display the TCIF growth curves obtained for different combinations of parameters. In all figures, TCIF growth curves are obtained for fixed values of r_L and r_H changing the parameters I_1, A, ϕ/I_A and W_A/I_A. Figures 1–5, which differ for the values of r_L and r_H ($r_L = 0.1$ and $r_H = 0.3$ in Fig. 1, $r_L = 0.1$ and $r_H = 0.6$ in Fig. 2, $r_L = 0.3$ and $r_H = 0.6$ in Fig. 3, $r_L = 0.3$ and $r_H = 0.9$ in Fig. 4, $r_L = 0.1$ and $r_H = 0.9$ in Fig. 5) are divided in six subplots, each subplot reports the growth curves obtained with a fixed value of the ratio W_A/I_A (the values reported in Table 4) and different values of I_1, A and ϕ/I_A. As a first important evidence, in Figs. 1–5, we observe that the TCIF cdfs obtained for different values of basin area A and rainfall intensity I_1 and keeping constant the ratios W_A/I_A and ϕ/I_A practically collapse into one curve. In these graphs, we grouped by colour all cdfs with the same value of ϕ/I_A (i.e. with the same Λ_q and coefficient of variation): in blue $\phi/I_A = 0.049$ ($\Lambda_q = 20$), in red $\phi/I_A = 0.742$ ($\Lambda_q = 10$), in black $\phi/I_A = 1.435$ ($\Lambda_q = 5$). In each subplot, the three groups of cdfs differ for both the scale and the shape factor.

In Tables 5–9, for a set of couples of r_L and r_H values, ($r_L = 0.1$ and $r_H = 0.3$ in Table 5, $r_L = 0.1$ and $r_H = 0.6$ in Table 6, $r_L = 0.3$ and $r_H = 0.6$ in Table 7, $r_L = 0.3$ and $r_H = 0.9$ in Table 8, $r_L = 0.1$ and $r_H = 0.9$ in Table 9), we report the values of the coefficient of skewness of such TCIF cdfs obtained with fixed values of W_A/I_A and

ϕ/I_A changing both the values of basin area $A = 10, 50, 100, 200, 500\,\text{km}^2$ and of rainfall intensity $I_1 = 10, 50\,\text{mm}\,\text{h}^{-1}$. Following the previous observation regarding the insensitivity of the coefficient of skewness to A and I_1, we report in each cell only the mean value and the standard deviation of the skewness coefficients obtained by considering the ensemble of ten cdfs obtained considering only the variability of basin area and rainfall intensity. The results show a standard deviation always significantly lower than the average.

Observing more carefully results reported in Tables 5–9, one may appreciate the effects of model parameters on skewness coefficient. In Table 5, the mean coefficient of skewness ranges from 1.608 to a maximum value of 2.452, for $r_L = 0.1$ and $r_H = 0.3$. In Table 6, the mean coefficient of skewness ranges from 1.595 to 3.417, for $r_L = 0.1$, $r_H = 0.6$. In Table 7, for $r_L = 0.3$, $r_H = 0.6$ the mean coefficient of skewness ranges from 1.540 to 1.826 which is the minimum peak of skewness observed over all the parameter sets. In Table 8, we have the minimum coefficient of skewness equal to 1.472 and a peak of skewness of 1.935 for $r_L = 0.3$, $r_H = 0.9$. In Table 9, for $r_L = 0.1$, $r_H = 0.9$ we have the minimum coefficient of skewness of 1.400 and a peak of skewness of 3.723 which is also the highest value observed over all the parameter sets. In general, comparing results of Tables 5–9, a strong relationship between skewness and permeability can be observed. In fact the minimum value of the coefficient of skewness is always observed for low permeability while soil storage may be either low or high. On the other hand a peak of skewness is always observed, for medium values of soil storage, and for medium or high values of permeability. In other words, the coefficient of skewness shows maximum values for medium-high values of permeability and medium values of soil storage. This is consistent with Table 2 being the skewness high when the two components of flood distribution can be clearly observed and distinguished.

In order to better understand the comparison among the different curves, accounting separately for the scale factor and the shape factor effects, the same cdfs shown in Figs. 1–5 are reported, respectively, in Figs. 6–10 with a different organization. In this case, all subplots report different TCIF cdfs that have a fixed ratio ϕ/I_A and variable values of ϕ/I_A (as described in the bottom part of Table 4), I_1 and A. Obviously, even in these figures the cdfs obtained for different values of I_1 and A collapse into one curve, but in these figures the colour code is used in order to identify different values of W_A/I_A. Since ϕ/I_A is fixed, in each of these subplots all curves have the same scale factor. Then the differences shown by the different values of W_A/I_A are all due to the curve shape factor, i.e. the coefficient of skewness. By comparing Figs. 6–10 one could notice that the minimum skewness is provided by a higher value of r_L (e.g. 0.3 in Figs. 8 and 9). On the other hand, the largest scatter is provided in Fig. 10 with a low value of r_L (0.1) and a high r_H (0.9).

Finally, the TCIF cdfs, having the same values of r_L and r_H, are grouped in Fig. 11a, b, c, d and e in order to provide a complete overview of the effects due to the parameters $I_1, A, W_A/I_A$ and ϕ/I_A. The scatter observed in Figs. 6–10 produces significant effects, in fact in the subplot 11b with the highest scatter in the shape factor the cdfs with different scale factor show a marked overlap. Subplot 11c has the lowest scatter in shape factor, while the difference in the scale factor, dominates the cdfs behaviour.

For the same values of $\Lambda_p = 21$ and $\varepsilon = 0.3$, we reported in Fig. 12 and Table 10 four cases obtained with $r_L = r_H = 0.05$, 0.1, 0.3 and 0.9. Results show that in this case all cdfs with the same value of ϕ/I_A and different values of I_1, A and also W_A/I_A collapse into one group of curves, with a practically null scatter. The mean value and the standard deviation of the coefficients of skewness are evaluated on a set of 60 cdfs obtained, for any value of ϕ/I_A, by combining the ratios $W_A/I_A = 1.098$, 2.302, 2.996, 3.912, 5.298, 6.908 (as in bottom part of Table 4) with the values of basin area $A = 10$, 50, 100, 200, 500 km^2 and the rainfall intensities $I_1 = 10$, 50 mm h^{-1}. Also in this case the standard deviation is always significantly smaller than the average skewness. Results in Table 10 show that the skewness always grows with permeability and higher skewness is obtained for lower values of $r_L = r_H$. The minimum value of the skewness is 1.235 and is obtained for the highest value of $r_L = r_H = 0.9$. This value which is also the minimum value observed over the entire dataset of simulations is not far from, but significantly higher, of the skeweness coefficient of a Gumbel distribution which is equal to 1.13955. Figure 13 shows the same growth curves of all subplots in Fig. 12 in order to show the overlap between different values of $r_L = r_H$.

Analogous evaluations were performed considering different values of Λ_p and ε, parameters that reflect respectively the rainfall coefficient of variation (Λ_p) and the average rainfall scaling with area (ε, see Eq. 8). In particular for $\Lambda_p = 75$ and $\varepsilon = 0.3$; $\Lambda_p = 21$ and $\varepsilon = 0.4$; $\Lambda_p = 40$ and $\varepsilon = 0.4$; in all cases the results confirm the behaviour displayed for $\Lambda_p = 21$ and $\varepsilon = 0.3$.

By the analysis of the overall results obtained from the entire dataset of cdfs and related coefficients of skewness, we found also another important evidence. A strong relationship exists between the coefficient of skewness and the parameters r_L and r_H, independently from the variability of all other parameters. As we report in Fig. 14, the values of the maximum coefficient of skeweness, obtained for different values of r_L and r_H, by varying the other parameters, show a strong linear dependence on the ratio r_H/r_L^2. On the other hand, Fig. 15 reports a dependence between the minimum coefficient of skewness and the product $r_H \times r_L$ obtained by varying $I_1, A, W_A/I_A$ and ϕ/I_A. In Figs. 14 and 15 we also show results obtained for several other couples of r_L and r_H reported in Table 11.

4 Conclusions

The sensitivity analysis performed over parameters of the TCIF distribution provides an interesting insight on the control that some physically based parameters have on the skewness coefficient. The main results are summarized in the following:

- the dimensionless ratios ϕ/I_A and W_A/I_A strongly affect the distribution skewness and the growth curve;
- for a fixed combination of the dimensionless ratios ϕ/I_A and W_A/I_A the skewness coefficient is independent from the basin area, A (ranging from 10 to 500 km^2),

HESSD
8, 5559–5604, 2011

and rainfall intensity per unit area, I_1 (ranging from 10 to 50 mm h^{-1}), in the range of variability investigated in this paper;

- for a fixed combination of the dimensionless ratios ϕ/I_A and W_A/I_A the skewness coefficient is also independent from Λ_p ranging from 21 to 75;
- for a fixed combination of the dimensionless ratios ϕ/I_A and W_A/I_A the skewness coefficient shows a significant dependence on the rainfall scaling coefficient ε;
- if $r_L = r_H$, the skewness coefficient (Cs) is independent from W_A: $\mathrm{Cs} = f(\phi/I_A)$;
- if $r_L \neq r_H$, the skewness coefficient depends on both ϕ and W_A: $\mathrm{Cs} = f(\phi/I_A, W_A/I_A)$;
- in all cases, for fixed ϕ/I_A the skewness coefficient assumes a local maximum increasing W_A/I_A;
- for a fixed value of Λ_p and ε, the maximum skewness increases with the ratio r_H/r_L^2;
- for a fixed value of Λ_p and ε, the combination $r_L = r_H$ produces low values of skewness which also decreases with r_L;
- for a fixed value of Λ_p and ε, the minimum skewness decreases with the product $r_L \times r_H$.

The above presented sensitivity analysis was performed assuming rainfall as Gumbel distributed. Hence the rainfall skew is always equal to 1.13955. The resulting flood skew is always higher than this and it reaches its maximum values when the probability of observing two different runoff components is high. For this purpose it is necessary that the permeability is not too low compared to average rainfall, so that it is significant for developing an ordinary component and it is necessary also that the soil storage is neither too low nor too high, compared to average rainfall. In fact, if soil storage is too low the second component is not distinguishable from the first component. If soil storage is too high, the second component becomes too rare and thus not significant for observable values. For fixed combination of other parameters and mainly r_L and r_H, by changing $I_1, A, \phi/I_A$ and W_A/I_A, it is possible to obtain a maximum value of C_s. Such a value is high as much as both r_L and r_L/r_H decrease, thus C_s shows a straight relationship with r_H/r_L^2. On the other hand the minimum values of C_s are obtained when, independently from the values of ϕ/I_A and W_A/I_A, $r_L = r_H$ in such a case there is no evidence of the second component. The condition $r_L = r_H$ can be obtained in real basins, for geomorphological reasons, for example when valleys are very steep and the average contributing area is always low. In such a case we may have two significant components but a skewness coefficient not very high.

Further research is needed for the case $k \neq 1$, i.e. when rainfall is not Gumbel distributed and may assume high skewness coefficient. In such a case a strong flood skewness could be expected even for single component runoff mechanisms.

Acknowledgements. This work was realized with support of PRIN Cubist – CoFin2007 of the MIUR (Italian Ministry of Instruction, University and Research).

References

Beven, K. J.: Towards the use of catchment geomorphology in flood frequency predictions, Earth Surf. Proc. Land., 12, 6–82, 1987.

Blazkova, S. and Beven. K. J.: Flood frequency estimation by continuous simulation for a catchment treated as ungauged (with uncertainty), Water. Resour. Res., (38)8, 1–14, 2002.

Blazkova, S. and Beven, K.: Flood frequency estimation by continuous simulation of subcatchment rainfalls and discharges with the aim of improving dam safety assessment in a large basin in the Czech Republic, J. Hydrol., 292, 153–172, 2004.

Bocchiola, D. and Rosso, R.: Use of a derived distribution approach for flood prediction in poorly gauged basins: A case study in Italy, Adv. Water Resour., 32, 1284–1296, 2009.

De Michele, C. and Salvadori, G.: On the derived flood frequency distribution: analytical formulation and the influence of antecedent soil moisture condition, J. Hydrol., 262, 245–258, 2002.
Eagleson, P. S.: Dynamics of flood frequency, Water Resour. Res., 8(4), 878–898, 1972.
Fiorentino, M. and Iacobellis, V.: New insights about the climatic and geologic control on the probability distribution of floods, Water Resour. Res., 37, 721–730, 2001.
Fiorentino, M., Manfreda, S., and Iacobellis, V.: Peak runoff contributing area as hydrological signature of the probability distribution of floods, Adv. Water Resour., 30, 2123–2134, 2007.
Fiorentino, M., Gioia, A., Iacobellis, V., and Manfreda, S.: Regional analysis of runoff thresholds behaviour in Southern Italy based on theoretically derived distributions, Adv. Geosc., 26, 139–144, 2011.
Franchini, M., Galeati, G., and Lolli, M.: Analytical derivation of the flood frequency curve through partial duration series analysis and a probabilistic representation of the runoff coefficient, J. Hydrol., 303, 1–15, 2005.
Gioia, A., Iacobellis, V., Manfreda, S., and Fiorentino, M.: Runoff thresholds in derived flood frequency distributions, Hydrol. Earth Syst. Sci., 12, 1295–1307, doi:10.5194/hess-12-1295-2008, 2008.
Gottschalk, L. and Weingartner, R.: Distribution of peak flow derived from a distribution of rainfall volume and runoff coefficient, and a unit hydrograph, J. Hydrol., 208, 148–162, 1998.
Iacobellis, V. and Fiorentino, M.: Derived distribution of floods based on the concept of partial area coverage with a climatic appeal, Water Resour. Res., 36(2), 469–482, 2000.
Iacobellis, V., Claps, P., and Fiorentino, M.: Climatic control on the variability of flood distribution, Hydrol. Earth Syst. Sci., 6, 229–238, doi:10.5194/hess-6-229-2002, 2002.
Iacobellis, V., Gioia, A., Manfreda, S., and Fiorentino, M.: Flood quantiles estimation based on theoretically derived distributions: regional analysis in Southern Italy, Nat. Hazards Earth Syst. Sci., 11, 673–695, doi:10.5194/nhess-11-673-2011, 2011.
Kusumastuti, D. I., Struthers, I., Sivapalan, M., and Reynolds, D. A.: Threshold effects in catchment storm response and the occurrence and magnitude of flood events: implications for flood frequency, Hydrol. Earth Syst. Sci., 11, 1515–1528, doi:10.5194/hess-11-1515-2007, 2007.
Loukas, A.: Flood frequency estimation by a derived distribution procedure, J. Hydrol., 255, 69–89, 2002.

McCuen, R. H. and Smith, E.: Origin of Flood Skew, J. Hydrol. Eng., 13, 771–775, doi:10.1061/(ASCE)1084-0699(2008)13:9(771), 2008.
McGrath, G. S., Hinz, C., and Sivapalan, M.: Temporal dynamics of hydrological threshold events, Hydrol. Earth Syst. Sci., 11, 923–938, doi:10.5194/hess-11-923-2007, 2007.
Merz, R. and Bloschl, G.: A regional analysis of event runoff coefficients with respect to climate and catchment characteristics in Austria, Water Resour. Res., 45, W01405, doi:10.1029/2008WR007163, January 2009.
NERC (Natural Environment Research Council): Flood studies report, Vol. I – Hydrologic studies, NERC, London, 1975.
Raines, T. H. and Valdes, J. B.: Estimation of flood frequencies for ungauged catchments, J. Hydrol. Eng., 119(8), 1138–1154, 1993.
Sivapalan, M., Wood, E. F., and Beven, K. J.: On hydrologic similarity, 3, A dimensionless flood frequency model using a generalized geomorphologic unit hydrograph and partial area runoff generation, Water Resour. Res., 26(1), 43–58, 1990.
Struthers, I. and Sivapalan, M.: A conceptual investigation of process controls upon flood frequency: role of thresholds, Hydrol. Earth Syst. Sci., 11, 1405–1416, doi:10.5194/hess-11-1405-2007, 2007.

HESSD
8, 5559–5604, 2011

Influence of soil parameters on the skewness coefficient

A. Gioia et al.

Table 1. Frequency of rainfall exceedance over different thresholds ϕ and W_A.

		Soil storage capacity (W_A)		
	$i > \phi$ / $i > W_A + \phi$	Low	Medium	High
Permeability (ϕ)	Low	frequent / frequent	frequent / occasional	frequent / rare
	Medium	occasional / occasional	occasional / rare	occasional / very rare
	High	rare / rare	rare / very rare	rare / extremely rare

HESSD
8, 5559–5604, 2011

Influence of soil parameters on the skewness coefficient

A. Gioia et al.

Table 2. Expected basin behaviour, in terms of presence and weight of the two components, based on a broad classification of the different thresholds ϕ and W_A.

		Soil storage capacity (W_A)		
	CDF type	Low	Medium	High
Permeability (ϕ)	Low	1 component	2 components (1st may be not relevant)	2 components (1st may be not relevant)
	Medium	1 component	2 components	2 components (2nd may be not observed)
	High	1 component	2 components (2nd may be not observed)	2 components (2nd may be not observed)

HESSD
8, 5559–5604, 2011

Influence of soil parameters on the skewness coefficient

A. Gioia et al.

Table 3. Mean annual number of events of the 2nd component (H-type response) based on different values of Λ_q and Λ_H/Λ_q.

		Λ_H					
Λ_q		Λ_H/Λ_q					
		1/3	1/10	1/20	1/50	1/200	1/1000
High	20	6.667	2.000	1.000	0.400	0.100	0.020
Medium	10	3.333	1.000	0.500	0.200	0.050	0.010
Low	5	1.667	0.500	0.250	0.100	0.025	0.005

HESSD
8, 5559–5604, 2011

Table 4. Values of dimensionless ratios ϕ/I_A (for $\Lambda p = 21$) and W_A/I_A, based on different values of Λ_q and Λ_H/Λ_q.

ϕ/I_A							
$\Lambda p = 21$		Λ_H/Λ_q					
Λ_q		1/3	1/10	1/20	1/50	1/200	1/1000
High	20	0.049	0.049	0.049	0.049	0.049	0.049
Medium	10	0.742	0.742	0.742	0.742	0.742	0.742
Low	5	1.435	1.435	1.435	1.435	1.435	1.435
W_A/I_A							
Λ_q		Λ_H/Λ_q					
		1/3	1/10	1/20	1/50	1/200	1/1000
High	20	1.098	2.302	2.996	3.912	5.298	6.908
Medium	10	1.098	2.302	2.996	3.912	5.298	6.908
Low	5	1.098	2.302	2.996	3.912	5.298	6.908

HESSD
8, 5559–5604, 2011

Influence of soil parameters on the skewness coefficient

A. Gioia et al.

Table 5. Mean and standard of skewness for $r_L = 0.1$, $r_H = 0.3$; A ranges from 10 to 500 km^2 and I_1 ranges from 10 to 50 mm h^{-1}.

Mean of Skewness						
	$W_A/I_A = 1.098$	$W_A/I_A = 2.302$	$W_A/I_A = 2.996$	$W_A/I_A = 3.912$	$W_A/I_A = 5.298$	$W_A/I_A = 6.908$
$\phi/I_A = 0.049$	1.858	2.252	2.260	2.053	1.743	1.612
$\phi/I_A = 0.742$	1.999	2.324	2.248	1.995	1.714	1.608
$\phi/I_A = 1.435$	2.225	2.452	2.308	2.039	1.792	1.707
Standard Deviation of Skewness						
	$W_A/I_A = 1.098$	$W_A/I_A = 2.302$	$W_A/I_A = 2.996$	$W_A/I_A = 3.912$	$W_A/I_A = 5.298$	$W_A/I_A = 6.908$
$\phi/I_A = 0.049$	0.025	0.066	0.082	0.077	0.049	0.034
$\phi/I_A = 0.742$	0.017	0.038	0.038	0.021	0.006	0.016
$\phi/I_A = 1.435$	0.011	0.018	0.010	0.009	0.028	0.035

HESSD
8, 5559–5604, 2011

Table 6. Mean and standard of skewness for r_L =0.1, r_H =0.6; A ranges from 10 to 500 km^2 and I_1 ranges from 10 to 50 mm h^{-1}.

Mean of Skewness						
	$W_A/I_A = 1.098$	$W_A/I_A = 2.302$	$W_A/I_A = 2.996$	$W_A/I_A = 3.912$	$W_A/I_A = 5.298$	$W_A/I_A = 6.908$
$\phi/I_A = 0.049$	1.595	2.268	2.832	3.124	2.565	1.858
$\phi/I_A = 0.742$	1.820	2.720	3.127	3.151	2.385	1.786
$\phi/I_A = 1.435$	2.188	3.155	3.417	3.172	2.325	1.837
Standard Deviation of Skewness						
	$W_A/I_A = 1.098$	$W_A/I_A = 2.302$	$W_A/I_A = 2.996$	$W_A/I_A = 3.912$	$W_A/I_A = 5.298$	$W_A/I_A = 6.908$
$\phi/I_A = 0.049$	0.011	0.233	0.060	0.102	0.108	0.057
$\phi/I_A = 0.742$	0.008	0.028	0.048	0.066	0.040	0.004
$\phi/I_A = 1.435$	0.007	0.023	0.035	0.035	0.002	0.028

HESSD

8, 5559–5604, 2011

HESSD
8, 5559–5604, 2011

Influence of soil parameters on the skewness coefficient

A. Gioia et al.

Table 7. Mean and standard of skewness for $r_L = 0.3$, $r_H = 0.6$; A ranges from 10 to 500 km^2 and I_1 ranges from 10 to 50 mm h^{-1}.

	Mean of Skewness					
	$W_A/I_A = 1.098$	$W_A/I_A = 2.302$	$W_A/I_A = 2.996$	$W_A/I_A = 3.912$	$W_A/I_A = 5.298$	$W_A/I_A = 6.908$
$\phi/I_A = 0.049$	1.562	1.638	1.615	1.578	1.549	1.540
$\phi/I_A = 0.742$	1.645	1.695	1.662	1.621	1.591	1.582
$\phi/I_A = 1.435$	1.805	1.826	1.785	1.741	1.712	1.703
	Standard Deviation of Skewness					
	$W_A/I_A = 1.098$	$W_A/I_A = 2.302$	$W_A/I_A = 2.996$	$W_A/I_A = 3.912$	$W_A/I_A = 5.298$	$W_A/I_A = 6.908$
$\phi/I_A = 0.049$	3.38E-03	6.21E-03	7.23E-03	7.99E-03	8.39E-03	8.51E-03
$\phi/I_A = 0.742$	2.67E-03	4.56E-03	5.18E-03	5.63E-03	5.86E-03	5.92E-03
$\phi/I_A = 1.435$	1.93E-03	3.15E-03	3.49E-03	3.72E-03	3.78E-03	3.83E-03

Table 8. Mean and standard of skewness for $r_L = 0.3$, $r_H = 0.9$; A ranges from 10 to 500 km^2 and I_1 ranges from 10 to 50 mm h^{-1}.

Mean of Skewness						
	$W_A/I_A = 1.098$	$W_A/I_A = 2.302$	$W_A/I_A = 2.996$	$W_A/I_A = 3.912$	$W_A/I_A = 5.298$	$W_A/I_A = 6.908$
$\phi/I_A = 0.049$	1.472	1.692	1.696	1.638	1.570	1.544
$\phi/I_A = 0.742$	1.585	1.779	1.755	1.680	1.610	1.586
$\phi/I_A = 1.435$	1.784	1.935	1.885	1.799	1.730	1.707
Standard Deviation of Skewness						
	$W_A/I_A = 1.098$	$W_A/I_A = 2.302$	$W_A/I_A = 2.996$	$W_A/I_A = 3.912$	$W_A/I_A = 5.298$	$W_A/I_A = 6.908$
$\phi/I_A = 0.049$	2.33E-03	5.16E-03	6.49E-03	7.62E-03	8.29E-03	8.51E-03
$\phi/I_A = 0.742$	1.85E-03	3.90E-03	4.76E-03	5.44E-03	5.80E-03	5.91E-03
$\phi/I_A = 1.435$	1.36E-03	2.80E-03	3.31E-03	3.64E-03	3.78E-03	3.83E-03

HESSD
8, 5559–5604, 2011

Table 9. Mean and standard of skewness for $r_L = 0.1$, $r_H = 0.9$; A ranges from 10 to 500 km^2 and I_1 ranges from 10 to 50 mm h^{-1}.

Mean of Skewness						
	$W_A/I_A = 1.098$	$W_A/I_A = 2.302$	$W_A/I_A = 2.996$	$W_A/I_A = 3.912$	$W_A/I_A = 5.298$	$W_A/I_A = 6.908$
$\phi/I_A = 0.049$	1.400	2.130	2.729	3.346	3.096	2.097
$\phi/I_A = 0.742$	1.611	2.585	3.185	3.565	2.888	1.962
$\phi/I_A = 1.435$	1.994	3.144	3.662	3.723	2.761	1.966
Standard Deviation of Skewness						
	$W_A/I_A = 1.098$	$W_A/I_A = 2.302$	$W_A/I_A = 2.996$	$W_A/I_A = 3.912$	$W_A/I_A = 5.298$	$W_A/I_A = 6.908$
$\phi/I_A = 0.049$	7.89E-03	2.37E-02	4.30E-02	8.60E-02	1.29E-01	7.67E-02
$\phi/I_A = 0.742$	6.01E-03	2.03E-02	3.78E-02	6.70E-02	6.33E-02	1.10E-02
$\phi/I_A = 1.435$	4.78E-03	1.82E-02	3.21E-02	4.53E-02	1.90E-02	2.11E-02

Discussion Paper | Discussion Paper | Discussion Paper | Discussion Paper |

HESSD

8, 5559–5604, 2011

Influence of soil parameters on the skewness coefficient

A. Gioia et al.

Table 10. Mean and standard of skewness for different values of $r_L = r_H$; A ranges from 10 to 500 km^2 and I_1 ranges from 10 to 50 $\mathrm{mm\,h}^{-1}$.

$r_L = r_H = 0.05$

	Mean of Skewness	Standard Deviation of Skewness
$\phi/I_A = 0.049$	1.597	4.39E-02
$\phi/I_A = 0.742$	1.631	3.92E-02
$\phi/I_A = 1.435$	1.743	3.26E-02

$r_L = r_H = 0.3$

	Mean of Skewness	Standard Deviation of Skewness
$\phi/I_A = 0.049$	1.538	8.70E-03
$\phi/I_A = 0.742$	1.580	6.01E-03
$\phi/I_A = 1.435$	1.701	3.90E-03

$r_L = r_H = 0.1$

	Mean of Skewness	Standard Deviation of Skewness
$\phi/I_A = 0.049$	1.574	2.92E-02
$\phi/I_A = 0.742$	1.579	1.94E-02
$\phi/I_A = 1.435$	1.684	3.74E-02

$r_L = r_H = 0.9$

	Mean of Skewness	Standard Deviation of Skewness
$\phi/I_A = 0.049$	1.235	3.16E-05
$\phi/I_A = 0.742$	1.264	7.07E-05
$\phi/I_A = 1.435$	1.377	7.38E-05

HESSD

8, 5559–5604, 2011

Title Page
Abstract | Introduction
Conclusions | References
Tables | Figures
◀| |▶
◀ ▶
Back | Close
Full Screen / Esc
Printer-friendly Version
Interactive Discussion

Table 11. Minimum and maximum skewness coefficient obtained for different values of r_L and r_H; for $\Lambda_p = 21$, and $\varepsilon = 0.3$ or $\varepsilon = 0.4$.

		$\varepsilon = 0.3$		$\varepsilon = 0.4$	
r_L	r_H	Cs max	Cs min	Cs max	Cs min
0.05	0.05	1.743	1.597	1.637	1.523
0.1	0.1	1.684	1.574	1.560	1.439
0.3	0.3	1.701	1.538	1.605	1.450
0.2	0.2	1.705	1.519	1.596	1.452
0.4	0.4	1.671	1.498	1.577	1.431
0.7	0.7	1.469	1.303	1.429	1.283
0.9	0.9	1.377	1.235	1.354	1.226
0.1	0.3	2.452	1.608	2.123	1.462
0.1	0.6	3.417	1.595	2.861	1.564
0.3	0.6	1.826	1.540	1.694	1.454
0.3	0.9	1.935	1.472	1.783	1.447
0.3	0.4	1.735	1.538	1.623	1.453
0.2	0.3	1.803	1.520	1.675	1.451
0.2	0.6	2.226	1.541	1.991	1.463
0.4	0.6	1.683	1.468	1.588	1.416
0.1	0.2	1.994	1.581	1.820	1.444
0.1	0.4	2.853	1.654	2.461	1.496
0.1	0.5	3.182	1.696	2.641	1.528
0.1	0.8	3.623	1.448	3.103	1.465
0.1	0.9	3.723	1.400	2.952	1.422
0.2	0.4	1.946	1.524	1.793	1.453
0.2	0.7	2.314	1.550	1.612	1.453
0.2	0.9	2.402	1.479	2.162	1.478
0.3	0.5	1.782	1.538	1.666	1.453
0.3	0.7	1.873	1.533	1.729	1.455
0.4	0.5	1.672	1.482	1.578	1.422
0.4	0.8	1.707	1.431	1.610	1.395
0.4	0.9	1.717	1.413	1.619	1.384

HESSD

8, 5559–5604, 2011

Influence of soil parameters on the skewness coefficient

A. Gioia et al.

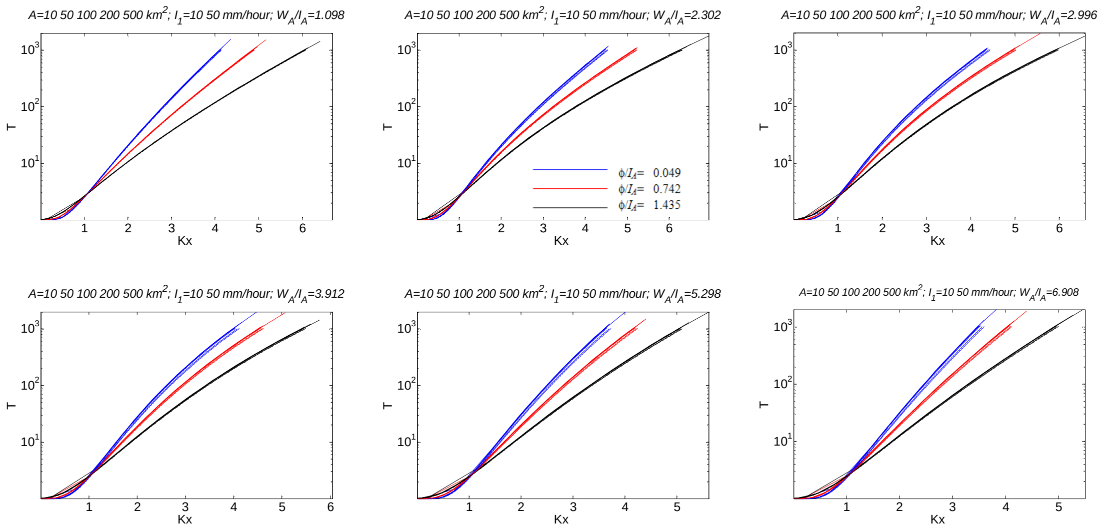

Fig. 1. Different growth curves obtained assigning a value to the ratio W_A/I_A and varying the values of I_1, A and ϕ/I_A for a fixed value of $r_L = 0.1$ and $r_H = 0.3$.

HESSD
8, 5559–5604, 2011

Influence of soil parameters on the skewness coefficient

A. Gioia et al.

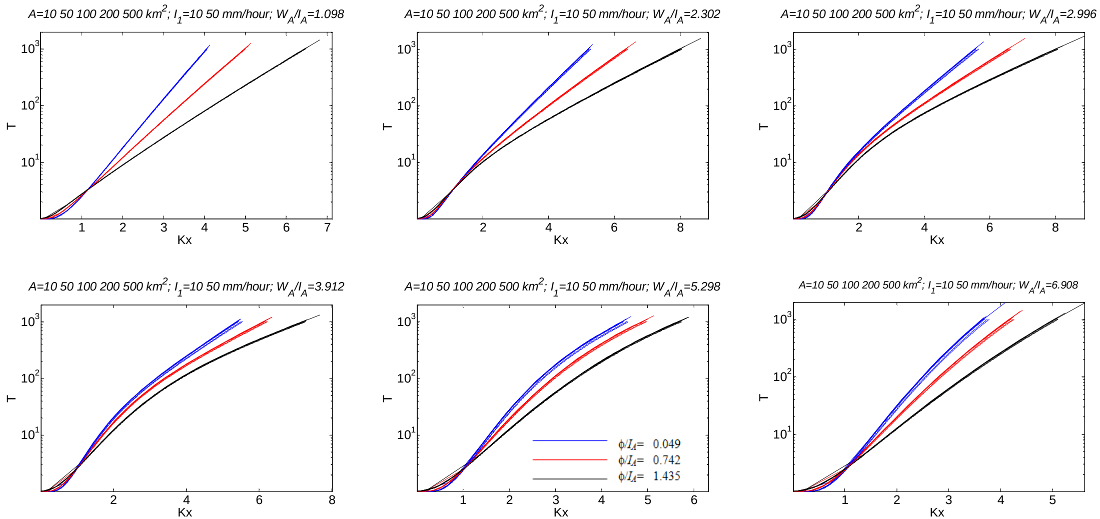

Fig. 2. Different growth curves obtained assigning a value to the ratio W_A/I_A and varying the values of I_1, A and ϕ/I_A for a fixed value of $r_L = 0.1$ and $r_H = 0.6$.

HESSD
8, 5559–5604, 2011

Influence of soil parameters on the skewness coefficient

A. Gioia et al.

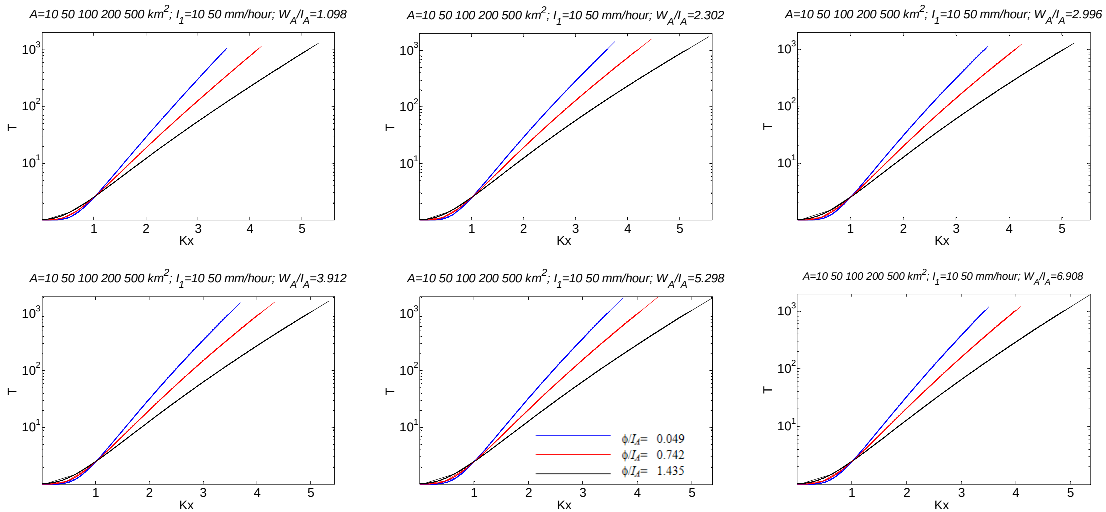

Fig. 3. Different growth curves obtained assigning a value to the ratio W_A/I_A and varying the values of I_1, A and ϕ/I_A for a fixed value of $r_L = 0.3$ and $r_H = 0.6$.

HESSD

8, 5559–5604, 2011

Influence of soil parameters on the skewness coefficient

A. Gioia et al.

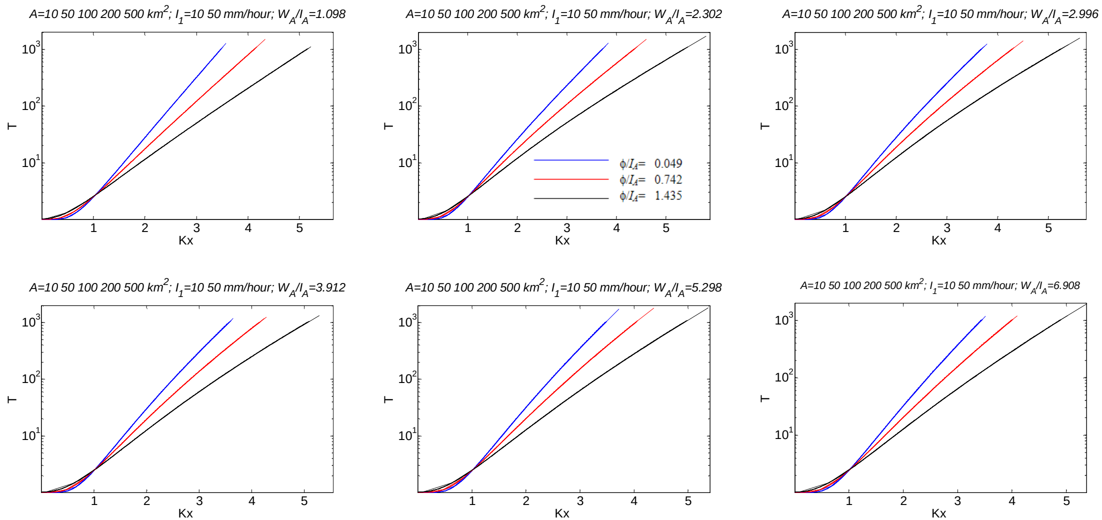

Fig. 4. Different growth curves obtained assigning a value to the ratio W_A/I_A and varying the values of I_1, A and ϕ/I_A for a fixed value of $r_L = 0.3$ and $r_H = 0.9$.

HESSD
8, 5559–5604, 2011

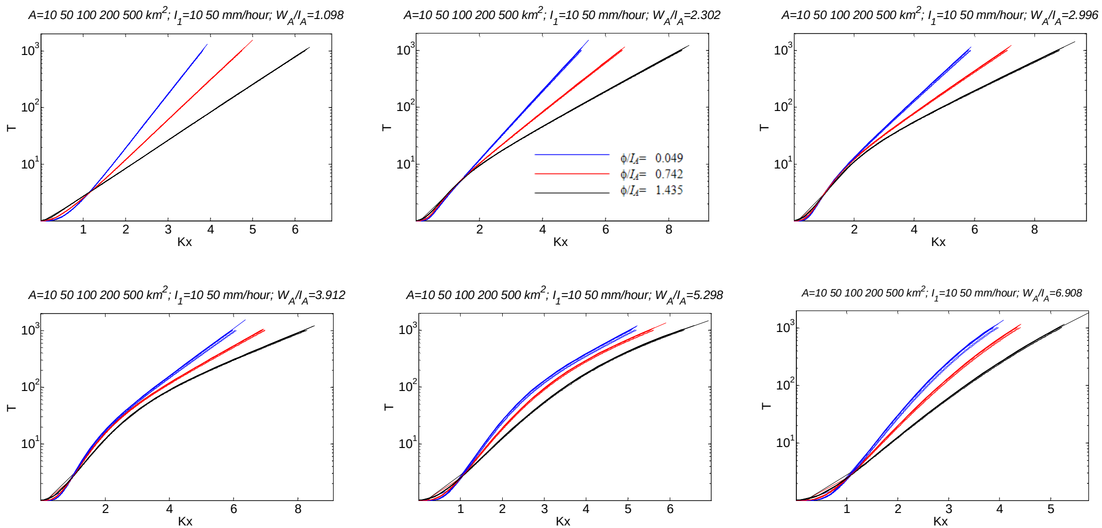

Fig. 5. Different growth curves obtained assigning a value to the ratio W_A/I_A and varying the values of I_1, A and ϕ/I_A for a fixed value of $r_L = 0.1$ and $r_H = 0.9$.

HESSD

8, 5559–5604, 2011

Influence of soil parameters on the skewness coefficient

A. Gioia et al.

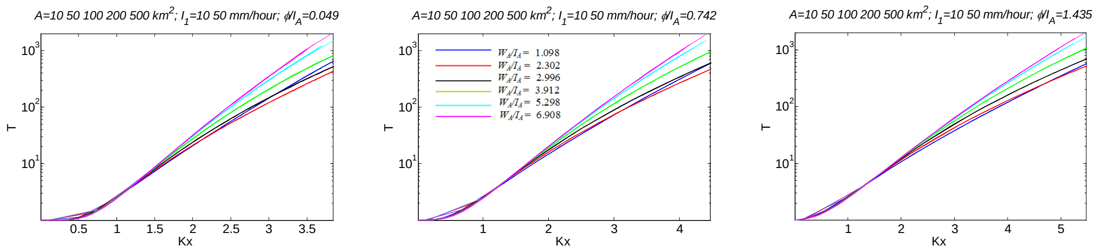

Fig. 6. Different growth curves obtained assigning a value to the ratio ϕ/I_A and varying the values of I_1, A and ϕ/I_A for a fixed value of $r_L = 0.1$ and $r_H = 0.3$.

HESSD

8, 5559–5604, 2011

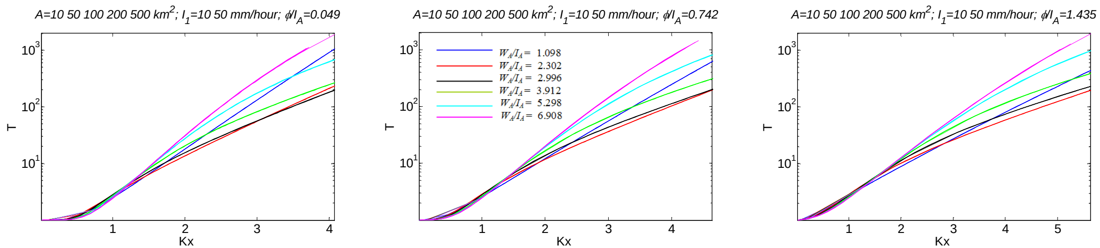

Fig. 7. Different growth curves obtained assigning a value to the ratio ϕ/I_A and varying the values of I_1, A and ϕ/I_A for a fixed value of $r_L = 0.1$ and $r_H = 0.6$.

HESSD
8, 5559–5604, 2011
Influence of soil parameters on the skewness coefficient
A. Gioia et al.

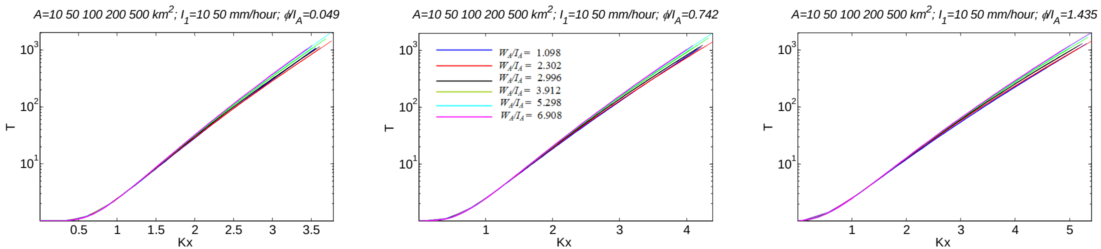

Fig. 8. Different growth curves obtained assigning a value to the ratio ϕ/I_A and varying the values of I_1, A and ϕ/I_A for a fixed value of $r_L = 0.3$ and $r_H = 0.6$.

HESSD
8, 5559–5604, 2011

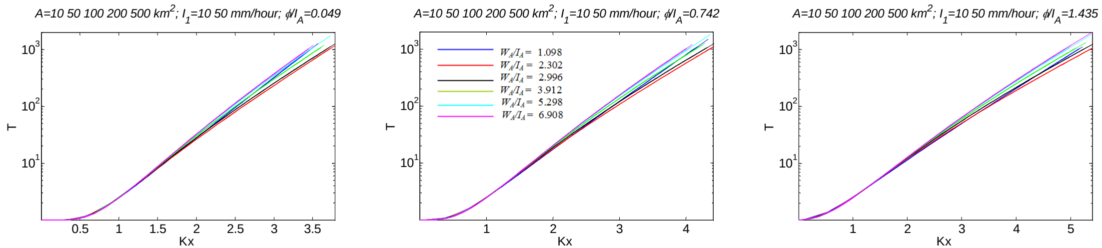

Fig. 9. Different growth curves obtained assigning a value to the ratio ϕ/I_A and varying the values of I_1, A and ϕ/I_A for a fixed value of $r_L = 0.3$ and $r_H = 0.9$.

HESSD
8, 5559–5604, 2011

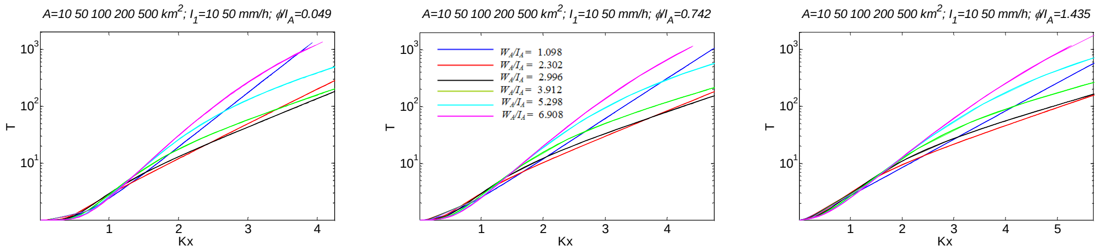

Fig. 10. Different growth curves obtained assigning a value to the ratio ϕ/I_A and varying the values of I_1, A and ϕ/I_A for a fixed value of $r_L = 0.1$ and $r_H = 0.9$.

HESSD
8, 5559–5604, 2011

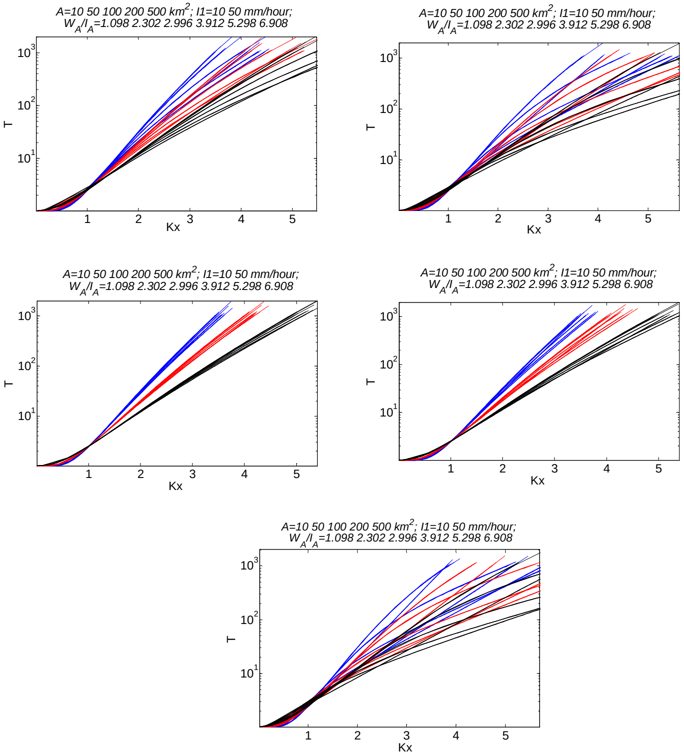

Fig. 11. **(a)** Different growth curves obtained varying the values of $I_1, A, W_A/I_A$ and ϕ/I_A for a fixed value of $r_L = 0.1$ and $r_H = 0.3$; **(b)** different growth curves obtained varying the values of $I_1, A, W_A/I_A$ and ϕ/I_A for a fixed value of $r_L = 0.1$ and $r_H = 0.6$. **(c)** Different growth curves obtained varying the values of $I_1, A, W_A/I_A$ and ϕ/I_A for a fixed value of $r_L = 0.3$ and $r_H = 0.6$. **(d)** Different growth curves obtained varying the values of $I_1, A, W_A/I_A$ and ϕ/I_A for a fixed value of $r_L = 0.3$ and $r_H = 0.9$. **(e)** Different growth curves obtained varying the values of $I_1, A, W_A/I_A$ and ϕ/I_A for a fixed value of $r_L = 0.1$ and $r_H = 0.9$.

HESSD
8, 5559–5604, 2011

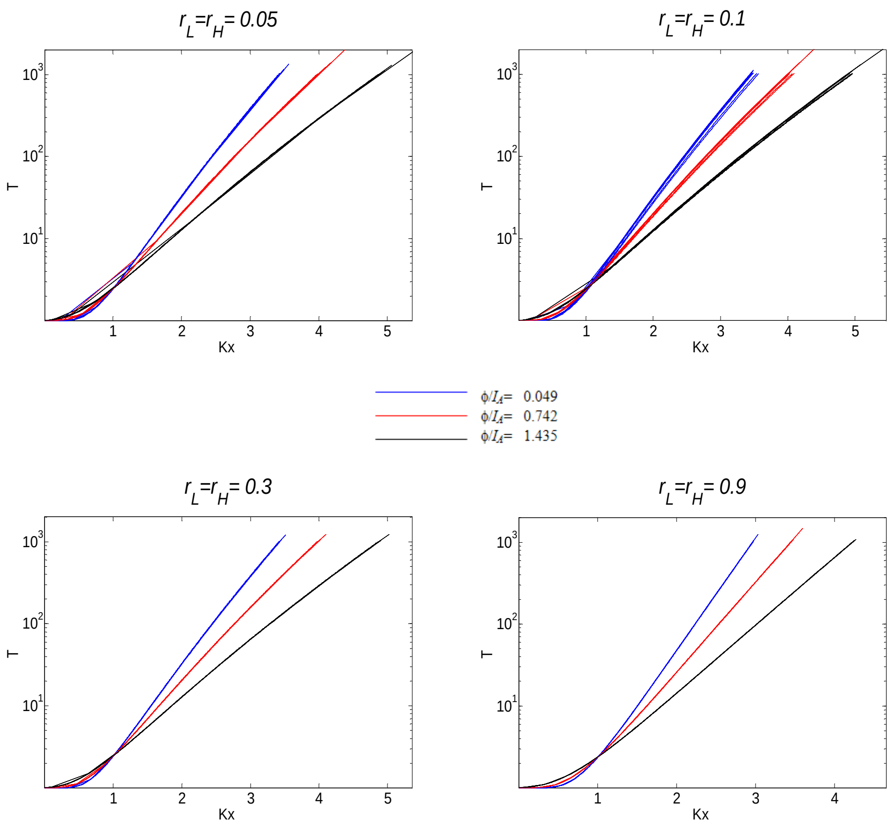

Fig. 12. Different growth curves obtained varying the values of I_1(10 and 50 m h^{-1}), A (10, 50, 200 and 500 km^2) W_A/I_A and ϕ/I_A as in Table 4, and $r_L = r_H$.

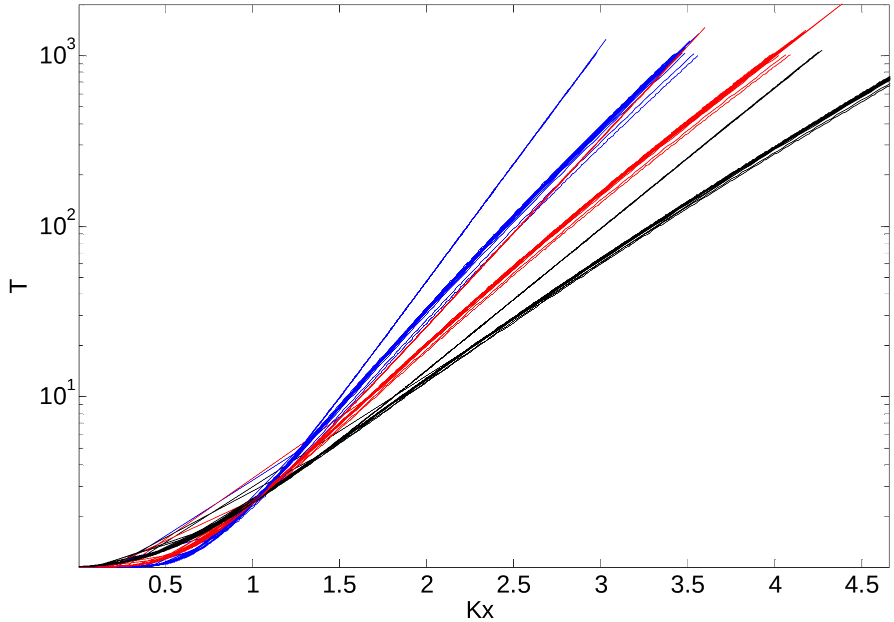

Fig. 13. Different growth curves obtained varying the values of I_1(10 and 50 m h^{-1}), A (10, 50, 200 and 500 km^2) W_A/I_A and ϕ/I_A as in Table 4, and $r_L = r_H$.

HESSD
8, 5559–5604, 2011

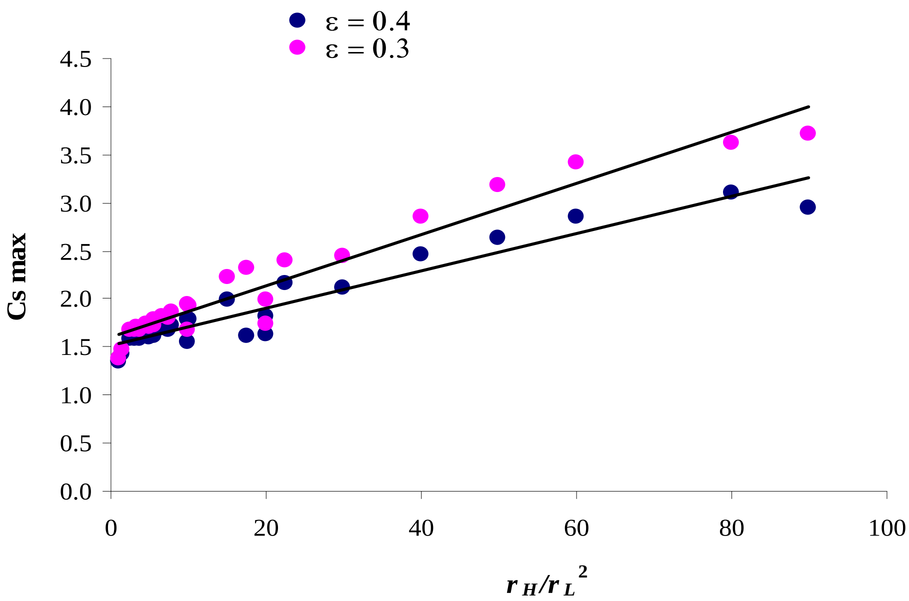

Fig. 14. Maximum skewness coefficient versus r_H/r_L^2, for $\Lambda_p = 21$, $\varepsilon = 0.3$ (magenta) and $\Lambda_p = 21$, $\varepsilon = 0.4$ (blue).

HESSD
8, 5559–5604, 2011

Influence of soil parameters on the skewness coefficient

A. Gioia et al.

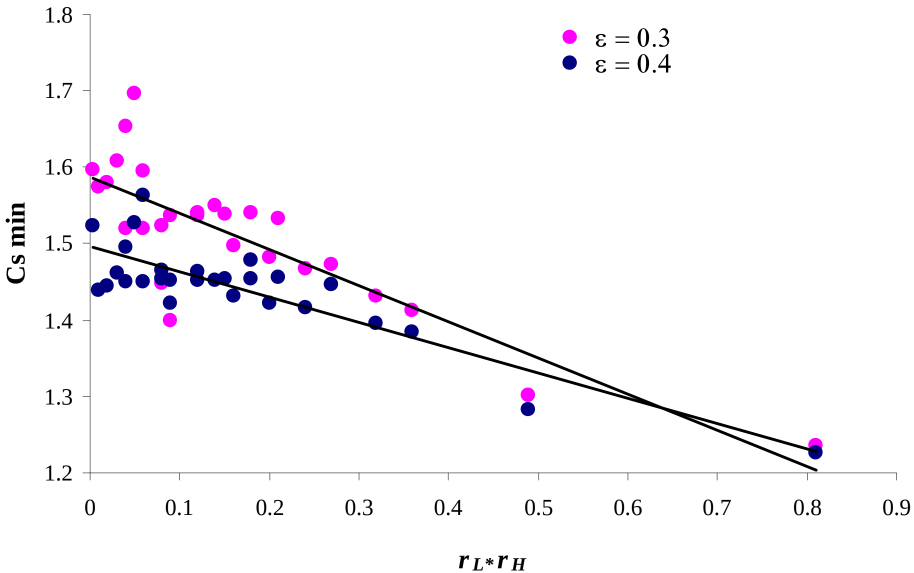

Fig. 15. Minimum skewness coefficient versus $r_L \cdot r_H$, for $\Lambda_p = 21$, $\varepsilon = 0.3$ (magenta) and $\Lambda_p = 21$, $\varepsilon = 0.4$ (blue).

HESSD
8, 5559–5604, 2011